ЖЭТФ, 1997, том 111, вып. 3, стр. 1001–1015

ON THE THEORY OF QUANTUM INTERFERENCE BETWEEN INELASTIC AND ELASTIC ELECTRON SCATTERING EVENTS

V. V. Rumyantsev, E. V. Orlenko, B. N. Libenson

Technical University of St. Petersburg
195251, St. Petersburg, Russia

Submitted 11 June 1996

The mechanism of weak localization of relatively fast electrons scattered with a fixed energy loss from disordered media is examined. The main focus of this paper is to put forward an explanation why coherent enhancement of electron scattering in the inelastic-scattering channel takes place at angles which differ from π. A simplified kinematic model is proposed to determine the basic properties of the weak localization of electrons in the inelastic scattering channel. The model reproduces easily the range of scattering angles typical of the weak localization of electrons with a fixed energy loss. The procedure does not require calculation of the contribution from the crossed diagrams. The results agree with those based on the dynamical theory associated with the calculation of the crossed and ladder diagrams. It is possible to follow the transition from the new type of weak localization to the ordinary weak localization with decreasing energy loss. The new-type weak localization is in agreement with the regular weak localization if the energy loss is approximately equal to the energy of an optical phonon.

1. INTRODUCTION

The weak localization of conduction electrons and backscattering enhancement of classical waves in disordered media have been studied extensively during the last few decades (see, for example [1–9]). The two phenomena, which are connected with the constructive interference of random wave fields, are closely related to each other. In the case of conduction electrons, coherent quantum mechanical backscattering can be regarded as a precursor of the exponential localization. It gives rise to a variety of quantum transport phenomena, particularly to the logarithmic increase in the resistance of metallic films with decreasing temperature which approaches absolute zero. In the case of electromagnetic waves and other classical fields, weak localization manifests itself in the enhancement of scattering in a narrow angular cone of width on the order of $1/(kl) \ll 1$ in the backward direction (k is the electron wave vector or the wave vector of a classical wave, and l is the mean free path).

Now we observe a partial shift of interest in the studies of weak localization from the problems of electron conductivity or elastic backscattering of light to new domains associated with the electron motion in disordered media. The discovery of universal conduction fluctuations has shifted the interest from average values of physical quantities to their variance and to the behavior of separate groups of electrons with fixed energies. Another point of interest is associated with the dissipation effects, because the inelastic scattering leads to the loss of phase memory of the wave function and suppresses the weak localization and the resistance fluctuations.

Finally, coherent phenomena are also of interest in the scattering of external particles (such as electrons) with a fixed energy incident on disordered samples. In contrast to electronic

measurements which can only measure the conductance of a system, experiments with the beams of intermediate-energy electrons have the advantage of measuring the angular and energy spectra of electrons for an experimental realization. In [10–12], the weak localization of external electrons (with energies from tens to thousands of electronvolts) has been studied. Neutrons have also been the subject of such a consideration [13]. According to those studies, coherent phenomena can be observed in the elastic backscattering of electrons, in spite of sufficiently high energies of external electrons.

In contrast with the scattering of electromagnetic waves, the interaction of an external energetic electron with a disordered medium leads, with high probability, to inelastic scattering. The effects of inelastic processes on the conductivity under weak localization have been studied extensively (for example, see [1, 2]). We now see a new wave of this activity. One method of treating inelastic processes when they occur only in an electron reservoir (coupled to a device without inelastic processes) was developed in [14, 15] and elsewhere subsequently. The quantum kinetic equation, which can be employed for describing quantum transport, has been derived under the assumption that the inelastic scattering is caused by noncorrelated point scatterers [16]. Much attention has been given to the effect of inelastic scattering on the observed coherent phenomena like the Aharonov–Bohm oscillations [17], conductance fluctuations [18, 19], persistent current [20], resonance behavior of the conductance [21], conductance of a disordered linear chain [22], and destruction of weak localization in inelastic scattering of particles [23]. We also point out an elegant experimental study [24], in which the authors tried to use the weak localization as a thermometer. Some studies are devoted to the effect of dissipation on the localization of classical fields. The reflection and transmission coefficients in the presence of absorption under the localization of classical fields have been considered in [25]. The effect of absorption on the wave transport has been studied in [26–35]. In many cases the absorption has been introduced as a uniform imaginary energy part. The common feature of those studies is that inelastic scattering destroys the phase memory and forbids the quantum interference effect.

In some cases, however, the inelastic processes do not lead to a phase memory loss. A very simple example was considered recently [36]. In that study the authors demonstrated the effect in which the electron-photon interaction in a ballistic microstructure plays the same role as the impurity scattering in disordered media. In the presence of an external electromagnetic field all relevant photons are coherent, and spatial interference in electron-photon scattering becomes allowed, despite the inelastic nature of the collisions. The electrons do not couple to a large number of degrees of freedom, and their phase memory is preserved. The interference effects are, therefore, certainly possible in the system, even though the electron scattering is inelastic.

The quantum interference can occur even if an electron undergoes a single inelastic scattering while interacting with an incoherent electromagnetic field. Because of a single inelastic collision, the electron loses a fixed energy, $\hbar\omega$, and finds itself in the so-called inelastic-scattering channel. The energy of this electron is different from the energy of the incident particles. It can escape the medium and then be detected. In addition to the single inelastic collision, the electron should undergo at least one elastic scattering before it leaves the medium through the same surface through which it penetrates the medium. There are two ways to realize this process, since it can either start or end with an inelastic collision. The interference of electron waves associated with these complementary processes has been proved [37, 38] to be constructive. It manifests itself in the enhancement of electron scattering through an angle which differs from π. The difference of this angle from π may be considerable. The new

coherent phenomenon is called «a new (or different) type of weak localization».

The ratio $\gamma/\omega < 1$ (where γ is the particle collision frequency, and $\hbar\omega$ is the particle energy loss) has been considered in [37–39]. Recently, the opposite limiting case $\gamma/\omega > 1$, which is closer to the usual weak localization (i.e., weak localization in the elastic-scattering channel), has been considered in [40,41]. In both cases the new type of weak localization appears to be clearly observable.

The main difference between the ordinary and the new weak localization is the typical electron scattering angle. The angular distribution of particles and radiation undergoing weak localization in a disordered medium can be found by calculating the contribution of the crossed (or so-called «fan») diagrams into an electron (radiation) cross section or density matrix. However, it is also useful to have a simple physical model explaining why coherent phenomena are particularly pronounced in particle scattering at certain angles. This approach is clear and enables us to evaluate the scattering angles without calculating the crossed diagrams. The main goal of the present article is to find the physical interpretation of the fact that constructive interference of the new weak localization is pronounced at scattering angles different from π.

In the case of the ordinary weak localization, there is a particular simple graphic method [2,42], which provides insight into the phenomenon and which explains why the angle π is specific for the regular weak localization. This method takes into account that an electron with a momentum $\mathbf{k}$ is scattered via two complementary series of intermediate scattering states $\mathbf{k} \to \mathbf{k}_1' \to \mathbf{k}_2' \to \ldots \to \mathbf{k}_{n-1}' \to \mathbf{k}_n' = -\mathbf{k}$ and $\mathbf{k} \to \mathbf{k}_1'' \to \mathbf{k}_2'' \to \ldots \to \mathbf{k}_{n-1}'' \to \mathbf{k}_n'' = -\mathbf{k}$ into the $-\mathbf{k}$ state. The momentum changes are $\mathbf{q}_1, \mathbf{q}_2, \ldots, \mathbf{q}_{n-1}, \mathbf{q}_n$ for the first series, and $\mathbf{q}_n, \mathbf{q}_{n-1}, \ldots, \mathbf{q}_2, \mathbf{q}_1$ for the second one. The amplitudes in the final state $-\mathbf{k}$ are identical, $A' = A'' = A$, and interfere constructively. This is because the complementary scattering series have the same momentum changes in opposite sequences.

The weak localization of electrons in the inelastic-scattering channel increases the electron scattering cross section at scattering angles different from π. Moreover, the effect is pronounced in a considerably wider range of angles than for the localization in the elastic-scattering channel. In this article we show that there exists a simple kinematic method which reproduces the range of scattering angles typical of the new type of weak localization. We explain the mechanism of particle localization with a fixed energy loss. The results obtained in the framework of our kinematic approach are compared with those based on the exact dynamical theory. The scattering angles typical of coherent scattering and calculated in the kinematic and dynamical approaches are in good agreement.

We shall also show that the localization of the new type turns into an ordinary localization in the limit of vanishing fixed energy loss.

2. KINEMATIC APPROACH TO DESCRIBE THE FEATURES OF WEAK LOCALIZATION

Let us consider a process in which the electron moving in a disordered medium undergoes elastic collisions and a single inelastic collision. The electron energy is assumed to be higher than the energies of the conduction electrons. The fixed energy loss $\hbar\omega$ of the electron occurs due to the inelastic collision. There are many sources of inelastic scattering, which provide a clearly distinguishable energy loss, for instance, plasmons and a number of electron atomic transitions.

In the regular weak localizations and in the new type of weak localizations the interference of the electron waves is described by crossed diagrams. In contrast with the ordinary weak

localization, one of the crossed lines in the new type of weak localization corresponds to the inelastic interaction, while the others correspond to elastic interaction with randomly distributed force centers. In accordance with Eq. (18) of [37], the crossed diagrams, together with the corresponding ladder diagrams, contribute to the scattering probability factor

$$\mathscr{S}(\omega,\chi)=(2\pi)^{-3}\int\limits_0^\infty dq_i\, q_i\, w_i(q_i,\omega)\mathscr{G}(q_i,\omega,\chi), \tag{1}$$

where χ is the electron scattering angle, $w_i(q_i,\omega)$ is the rate of inelastic scattering accompanied by excitation of the medium with a momentum q_i and energy $\hbar\omega$. The function $\mathscr{G}$ is given by

$$\mathscr{G}(q_i,\omega,\chi)=\hbar^2\int d\Omega_{\mathbf{q}_i}\,|G(\mathbf{k}-\mathbf{q}_i,E_k-\hbar\omega)+G(\mathbf{k}-\mathbf{Q}+\mathbf{q}_i,E_k)|^2\,. \tag{2}$$

Here $G(\mathbf{k}-\mathbf{q}_i,E_k-\hbar\omega)$ and $G(\mathbf{k}-\mathbf{Q}+\mathbf{q}_i,E_k)$ are the electron Green's functions. The former describes electron motion between the inelastic and elastic scattering events and the latter refers to the process with the opposite sequence of events. E_k and $\mathbf{k}$ are the initial energy and momentum of an incident electron, respectively; $\mathbf{Q}=\mathbf{q}_i+\mathbf{q}_e$ is the total momentum transfer to the medium, and $\mathbf{q}_e$ corresponds to the elastic scattering. The integration in Eq. (2) is performed over possible orientations of $\mathbf{q}_i$. Equation (2) can be rewritten in the form

$$\mathscr{G}(q_i,\omega,\chi)=\int d\Omega_{\mathbf{q}_i}\left|\frac{1}{\mathbf{vq}_i-\omega-\hbar q_i^2/2m-i\gamma}+\frac{1}{\omega-\mathbf{v}'\mathbf{q}_i-\hbar q_i^2/2m-i\gamma}\right|^2. \tag{3}$$

Here we assume that the electron energy is $E_k=\hbar^2k^2/2m$, $\mathbf{v}$ and $\mathbf{v}'$ are the electron velocities in the initial and final states, respectively, and γ is the electron collision frequency.

The function (3) is convenient for studying the weak localization since it describes the propagation of electron waves between collisions. Equation (3) contains three terms. The squared absolute value of the first Green's function gives the contribution of a ladder-type diagram and describes the process in which the first collision is inelastic. The squared absolute value of the second Green's function corresponds to a ladder-type diagram for the case in which the inelastic collision is the last collision. In both cases the expressions are independent of the electron-scattering angle, $\chi=\cos^{-1}(\mathbf{vv}'/vv')$. There is also the third term, which contains the product of the first and second Green's functions. It corresponds to the crossed diagrams and describes the interference of two electron waves which propagate along the same path in opposite directions. The integration over $\Omega_{\mathbf{q}_i}$ in this term does not kill the χ-dependence that describes the weak localization. The function $\mathscr{G}$ describes it at a fixed length of $\mathbf{q}_i$, while Eq. (1) is appropriate if the length of $\mathbf{q}_i$ is not fixed.

If an inelastic collision occurs between two elastic collisions, the weak localization does not exist [38]. It was also shown [38] that elastic multiple scattering at arbitrary angles does not change the angular dependence determined by the functions $\mathscr{G}$ and $\mathscr{S}$.

The squared absolute value of the first Green's function in Eq. (3) at small γ can be represented in the form

$$\left|\frac{1}{E_k-E_{\mathbf{k}-\mathbf{q}_i}-\hbar\omega-i\gamma}\right|^2\simeq\frac{\pi}{\hbar\gamma}\delta(E_k-E_{\mathbf{k}-\mathbf{q}_i}-\hbar\omega). \tag{4}$$

The squared absolute value of the second Green's function in Eq. (3) can be written similarly. The term in the integrand of Eq. (3) which describes the interference has the form

$$\frac{1}{(E_k - E_{\mathbf{k}-\mathbf{q}_i} - \hbar\omega - i\gamma)(E_k - E_{\mathbf{k}-\mathbf{Q}+\mathbf{q}_i} + i\gamma)} + \frac{1}{(E_k - E_{\mathbf{k}-\mathbf{Q}+\mathbf{q}_i} - i\gamma)(E_k - E_{\mathbf{k}-\mathbf{q}_i} - \hbar\omega + i\gamma)}. \quad (5a)$$

It is evident that the ratio of Eq. (5a) to Eq. (4) is proportional to the small quantity γ. We can assume, therefore, that the frequency γ in the denominators of Eq. (5a) is (as a first approximation) an infinitesimal quantity. This enables us to rewrite Eq. (5a) in the form

$$\left[\mathscr{P}\frac{1}{E_k - E_{\mathbf{k}-\mathbf{q}_i} - \hbar\omega} + i\pi\delta(E_k - E_{\mathbf{k}-\mathbf{q}_i} - \hbar\omega)\right]\left[\mathscr{P}\frac{1}{E_k - E_{\mathbf{k}-\mathbf{Q}+\mathbf{q}_i}} - i\pi\delta(E_k - E_{\mathbf{k}-\mathbf{Q}+\mathbf{q}_i})\right] +$$
$$+ \left[\mathscr{P}\frac{1}{E_k - E_{\mathbf{k}-\mathbf{Q}+\mathbf{q}_i}} + i\pi\delta(E_k - E_{\mathbf{k}-\mathbf{Q}+\mathbf{q}_i})\right]\left[\mathscr{P}\frac{1}{E_k - E_{\mathbf{k}-\mathbf{q}_i} - \hbar\omega} - i\pi\delta(E_k - E_{\mathbf{k}-\mathbf{q}_i} - \hbar\omega)\right]. \quad (5b)$$

An estimate reveals that in Eq. (5a) the ratio of the terms containing the product of two delta functions to the terms which contain the principal values is

$$\frac{\hbar\omega}{vq_c}\frac{k}{q_c}. \quad (6)$$

Here q_c is the maximum momentum q_i (for example, the cutoff plasmon momentum). As long as $k \gg q_c$, the contribution of the product of the delta functions is dominant. This means that although the quantum transport generally (and the weak localization specifically) occurs due to such electron collisions at which every next scattering begins before the end of the previous one, weak localization permits (to the first approximation) a physical interpretation, which starts from the analysis of the consequences of the simultaneous satisfaction of the two conditions,

$$E_k - E_{\mathbf{k}-\mathbf{Q}+\mathbf{q}_i} = 0 \quad \text{and} \quad E_k - E_{\mathbf{k}-\mathbf{q}_i} - \hbar\omega = 0. \quad (7)$$

These conditions come from the two delta functions and have the meaning of energy momentum conservation. An analysis based on Eqs. (7) is called the kinematic method in the theory of weak localization.

Below we compare the results of the kinematic analysis with the so-called dynamic results of the exact theory. We shall prove that the kinematic approach reproduces the angular properties of the weak localization with fairly good accuracy.

Let us rewrite Eqs. (7) in the form

$$E_{k'} - E_{\mathbf{k}-\mathbf{q}_i} = 0, \quad (8)$$

$$E_k - E_{\mathbf{k}-\mathbf{q}_e} = 0, \quad (9)$$

and show that the vectors $\mathbf{q}_i$ and $\mathbf{q}_e$, the momentum transfers during the inelastic and elastic collisions, are reciprocal orthogonal vectors.

Subtracting Eq. (8) from Eq. (9), we have

$$(\mathbf{k} - \mathbf{k}')(\mathbf{k} + \mathbf{k}') = (\mathbf{q}_i - \mathbf{q}_e)(2\mathbf{k} - \mathbf{q}_i - \mathbf{q}_e). \quad (10)$$

From Eq. (9) we obtain $q_e^2 = 2\mathbf{k}\mathbf{q}_e$. Since $\mathbf{Q} = \mathbf{k} - \mathbf{k}' = \mathbf{q}_i + \mathbf{q}_e$, we obtain

$$2\mathbf{k}(\mathbf{Q} - \mathbf{q}_i - \mathbf{q}_e) = Q^2 - q_i^2 - q_e^2. \quad (11)$$

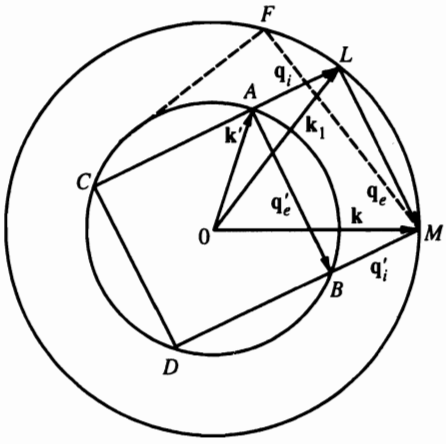

Fig. 1. Kinematic diagram of the sequence of events which give rise to a weak localization

Since $\mathbf{Q} = \mathbf{q}_i + \mathbf{q}_e$, we obtain $Q^2 = q_i^2 + q_e^2$. Therefore,

$$\mathbf{q}_i\mathbf{q}_e = 0. \tag{12}$$

Let us now represent graphically the sequence of events which give rise to a new type of weak localization. The circles in Fig. 1 have the radii $R = k$ and $R' = k' = \sqrt{k^2 - 2m\hbar^{-1}\omega}$, respectively. The radii coincide with the lengths of the electron wave vectors in the initial and final states. Let us first consider the case in which the first collision is elastic. For brevity, we denote this process as $\langle m, \mathbf{k}'|H_iGH_e|n, \mathbf{k}\rangle$. Here m and n correspond to the initial and final states of the medium. The end of the vector $\mathbf{q}_e$, the momentum transfer during the elastic scattering (which may involve multiple elastic scattering), touches the circle R , so that the electron wave vector becomes equal to $\mathbf{k}_1$ as a result of elastic scattering. The following event of the scattering is an inelastic collision with a momentum transfer $\mathbf{q}_i$, and the condition $\mathbf{q}_i\mathbf{q}_e = 0$ is satisfied. The vector $\mathbf{q}_i$ connects the end of the vector $\mathbf{k}_1$ with the point A on the circle $R' = k'$ (where the end of the vector $\mathbf{k}'$ rests). The energy of the final state electron is lower by $\hbar\omega$ than the energy of the initial state.

In the complementary scattering process $\langle m, \mathbf{k}'|H_eGH_i|n, \mathbf{k}\rangle$ the particle first loses its energy and only then undergoes the elastic scattering. The interference between two realizations of the scattering process is effective if the wave vectors transferred during inelastic scattering in each realization are parallel and if they have the same lengths. Therefore, the momentum transfer $\mathbf{q}_i'$ in the event of inelastic scattering in the process $\langle m, \mathbf{k}'|H_eGH_i|n, \mathbf{k}\rangle$ is shown with the segment that connects the end of the vector $\mathbf{k}$ and the point B on the circle $R' = k'$, where the vector $\mathbf{q}_i'$ is perpendicular to the vector $\mathbf{q}_e$. The vector $\mathbf{q}_e'$ in the process under consideration is shown with the segment AB. The vectors $\mathbf{q}_e$ and $\mathbf{q}_i$ in the process $\langle m, \mathbf{k}'|H_iGH_e|n, \mathbf{k}\rangle$ and the vectors $\mathbf{q}_i'$ and $\mathbf{q}_e'$ in the process $\langle m, \mathbf{k}'|H_eGH_i|n, \mathbf{k}\rangle$ convert the vector $\mathbf{k}$ to $\mathbf{k}'$.

As can be seen from Fig. 1, there is the other set of vectors $\mathbf{q}_i, \mathbf{q}_e$ and $\mathbf{q}_i', \mathbf{q}_e'$. In this case $\mathbf{q}_i$ connects the point C (at the end of $\mathbf{k}'$) with the end of $\mathbf{k}_1$. The segment CD and the segment joining the point D and the end of $\mathbf{k}$ define $\mathbf{q}_e'$ and $\mathbf{q}_i'$.

As a rule, the two sets of solutions, which correspond to the segments AB and CD, cannot be realized simultaneously. It is obvious that a solution concerned with the existence of the segment CD corresponds to the length $\mathbf{q}_i$,

$$q_i = \sqrt{k^2 - (q_e/2)^2} + \sqrt{k'^2 - (q_e/2)^2},$$

and to the electron-scattering angle,

$$\chi = \frac{\pi}{2} + \sin^{-1}\left(\frac{q_e}{2k}\right) + \sin^{-1}\left(\frac{q_e}{2k'}\right),$$

so that $\pi/2 \leq \chi \leq \pi$.

Therefore,

$$q_i^2 = k^2 + k'^2 + 2kk' \sin\chi, \tag{13}$$

$$q_e^2 = \frac{(2kk' \cos\chi)^2}{k^2 + k'^2 + 2kk' \sin\chi}. \tag{14}$$

It is evident that $q_i/q_e > 1$, an inequality that is difficult to realize. For example, in the case of plasmon excitations there is a cutoff vector $q_i = q_{ic} = \omega v_F^{-1}$ (where v_F is the electron Fermi velocity), and the probability of plasmon excitation with $q_i > q_{ic}$ is zero. In other cases of inelastic scattering the processes with small momentum transfers are also probable. However, when taking the limit of the ordinary weak localization ($k' \to k$), the solution of Eqs. (13) and (14) corresponds to the correct description of the process. When the ratio $\hbar\omega/E$ is small, we have

$$\cos\chi = -1 + \frac{1}{8\left[(2k/q_e)^2 - 1\right]}\left(\frac{\hbar\omega}{E}\right)^2, \tag{15}$$

and $\chi \to \pi$ as $\hbar\omega \to 0$.

When we consider the new type of weak localization, the solution associated with small momentum transfers $\mathbf{q}_i$ is realized. In this case the interference conforms to the rectangle with the vortices $ABLM$. According to Fig. 1, the dependence of the length of the vector $\mathbf{q}_i$ on χ has the form

$$q_i = \sqrt{k^2 - (q_e/2)^2} - \sqrt{k'^2 - (q_e/2)^2}, \tag{16}$$

and

$$\chi = \sin^{-1}\left(\frac{q_e}{2k}\right) + \sin^{-1}\left(\frac{q_e}{2k'}\right). \tag{17}$$

From Eqs. (16) and (17) we obtain

$$q_e^2 = \frac{(2kk' \sin\chi)^2}{k^2 + k'^2 + 2kk' \cos\chi}, \tag{18}$$

$$q_i = \frac{2m\omega}{\hbar\sqrt{k^2 + k'^2 + 2kk' \cos\chi}}. \tag{19}$$

We see from Eq. (19) that

$$\cos\chi = -\frac{k^2 + k'^2}{2kk'} + \frac{2\omega^2}{vv'q_i^2}. \tag{20}$$

This expression determines the electron-scattering angle under weak localization at different values of $\mathbf{q}_i$, the inelastic momentum transfer.

If $k - k' \ll k$, then

$$\cos\chi = -1 + \frac{2\omega^2}{v^2 q_i^2} \quad \text{or} \quad \cos\frac{\chi}{2} = \frac{\omega}{vq_i}.$$

It is convenient to rewrite them as

$$\chi = 2\cos^{-1}\left(\frac{\omega}{vq_i}\right). \tag{21}$$

If the electron scattering excites the electromagnetic waves (longitudinal or transverse), Eq. (21) can be interpreted as the condition of the electron scattering through the double Čerenkov angle. This circumstance was pointed out in [37].

There is a top value of the vector $\mathbf{q}_e$ (this vector is represented by the dashed line MF) at which the vector $\mathbf{q}_i$ drawn from the point F perpendicularly to the segment MF ceases to cross the inner circle. Accordingly, it is impossible to expect the new type of weak localization to be at electron-scattering angles close to π. We see from the geometric consideration that the top scattering angle is

$$\chi_0 = \pi - \cos^{-1}\left(1 - \frac{\hbar\omega}{2E}\right). \tag{22}$$

Therefore, we obtain

$$q_{i0} = k\sin\chi_0 = \sqrt{2m\omega\hbar^{-1}}. \tag{23}$$

The new type of weak localization takes place only if $q_i < q_{i0}$.

Now we can determine the range of scattering angles of the electrons that undergo weak localization for different types of medium excitations. When a bulk plasmon is excited and its wave vector is in the range

$$\frac{\omega_p}{v} < q_i < q_c = \frac{\omega_p}{v_F},$$

the coherent phenomena at electron scattering occur at

$$0 < \chi < 2\cos^{-1}(v_F/v). \tag{24}$$

The range of wave vectors of the transverse electromagnetic waves (at the Čerenkov excitation) is

$$\frac{\omega}{v} < q_i < \frac{\omega}{c}\sqrt{\epsilon}.$$

The most intense scattering will then occur in the range of scattering angles

$$0 < \chi < 2\cos^{-1}\left(\frac{c}{v\sqrt{\epsilon}}\right). \tag{25}$$

In the case of excitation and ionization of atoms [37] we have

$$q_i \simeq \frac{e\sqrt{Z}}{|d_{x\ mn}|},$$

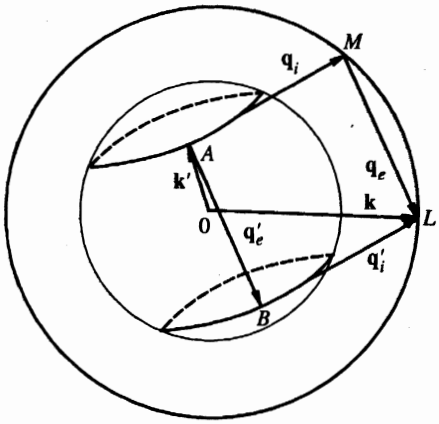

Fig. 2. Three-dimensional diagram of the realization of constructive interference

where Z is the atomic number, and $d_{x\ mn}$ is the matrix element of the atomic dipole for excitation from the ground state n to the upper state m. Therefore, the coherent phenomena at electron scattering will be pronounced at

$$\chi \simeq 2\cos^{-1}\left(\frac{\omega|d_{x\ mn}|}{ev\sqrt{Z}}\right). \tag{26}$$

For an optical-phonon excitation, the weak localization is effective when

$$\frac{\omega_{ph}}{v} < q_i < \frac{\sqrt{2m\omega_{ph}}}{k} \ll |\mathbf{G}|$$

($\mathbf{G}$ is the reciprocal lattice vector). The appropriate range of the electron-scattering angles is

$$0 < \chi < 2\cos^{-1}\left(\sqrt{\hbar\omega/4E}\right). \tag{27}$$

Until now we have assumed that every vector in Fig. 1 lies in the same plane. However, the vector $\mathbf{q}_i$, which is perpendicular to $\mathbf{q}_e$ does not necessarily lie in the plane of the vectors $\mathbf{k}$ and $\mathbf{q}_e$. If the vectors $\mathbf{q}_i, \mathbf{q}_e, \mathbf{q}'_i, \mathbf{q}'_e, \mathbf{k}$, and $\mathbf{k}'$ are situated as shown in Fig. 2, the complementary scattering processes will be accompanied by a constructive interference. In this case the ends of the vectors $\mathbf{q}_i$ and $\mathbf{q}'_i$ are situated on the circles formed by intersection of the inner sphere $R' = k'$ and the planes which are perpendicular to $\mathbf{q}_e$ and pass through the points L and M. The vectors $\mathbf{q}_i$ and $\mathbf{q}'_i$ form the «fan»

$$\frac{\omega\sqrt{2}}{v\sqrt{1-\cos\chi}} < q_i < \min\left[\sqrt{\frac{2m\omega}{\hbar^2}}, q_{i\ max}\right]. \tag{28}$$

Instead of Eq. (15) in this case we have

$$\cos\chi = -1 + \frac{1}{8\left[(2k/q_e)^2 - 1\right]\cos\phi}\left(\frac{\hbar\omega}{E}\right)^2, \tag{29}$$

where ϕ is the azimuthal angle (in the plane perpendicular to $\mathbf{k}$) between the vectors $\mathbf{k}'$ and $\mathbf{q}_e$. Although the kinematic diagram of the realization of effective interference is now three-dimensional, our conclusions about the interference mechanism and about the features of electron-scattering angles remain valid.

3. DYNAMICAL APPROACH FOR THE DESCRIPTION OF THE NEW TYPE OF WEAK LOCALIZATION

Although the description of weak localization requires, first of all, the contribution from the poles of the Green's functions in Eq. (3), the contribution from the principal value might modify the results of the previous section. In addition, we shall consider the uncertainty of the radii of the spheres in Figs. 1 and 2 due to the image potential of the medium. The uncertainty is $\kappa \simeq \sqrt{2m}U'[2\hbar\sqrt{E}]^{-1}$, where U' is the image potential mentioned above.

Moreover, the momentum transfer $\mathbf{q}_i$ usually is not fixed in experiments. Hence we should perform integration over $\mathbf{q}_i$. It is convenient to introduce the function

$$M(\chi) = \frac{\int\limits_0^{k+k'} dq_i\, q_i^2 w_i(q_i,\omega)\mathcal{G}_c(q_i,\omega,\chi)}{\int\limits_0^{k+k'} dq_i\, q_i^2 w_i(q_i,\omega)\mathcal{G}_L(q_i,\omega)}, \tag{30}$$

which is called the degree of coherency. Equations (12), (18), and (19) in [37] clarify the definition of $M(\chi)$. In Eq. (30) $w_i(q_i,\omega)$ is the rate of excitation of a state with energy $\hbar\omega$ and momentum $\mathbf{q}_i$.

The functions $\mathcal{G}_c$ and $\mathcal{G}_L$ occur due to the crossed and ladder diagrams; and they are defined as

$$\mathcal{G}_c(q_i,\omega,\chi) = 2\ \mathrm{Re} \int d\Omega_{\mathbf{q}} \frac{1}{(\mathbf{vq}_i - \omega - \hbar q_i^2/2m + i\gamma)\,(\omega - \mathbf{v}'\mathbf{q}_i - \hbar q_i^2/2m - i\gamma)}, \tag{31}$$

$$\mathcal{G}_L(q_i,\omega) = \int d\Omega_{\mathbf{q}} \left\{ \frac{1}{(\mathbf{vq}_i - \omega - \hbar q_i^2/2m)^2 + \gamma^2} + \frac{1}{(\omega - \mathbf{vq}_i - \hbar q_i^2/2m)^2 + \gamma^2} \right\}. \tag{32}$$

Here the damping is $\gamma = \kappa v$.

To analyze the weak localization during excitation of the long-wavelength medium states, e.g., of plasmons or optical phonons, it is convenient to write $w_i(q_i,\omega)$ as follows:

$$w_i(q_i,\omega) = \mathcal{F}(\omega) q_i^{-2}\, \theta(q_{i\ max} - q_i).$$

The function $\mathcal{F}(\omega)$ is the long-wavelength limit of the imaginary part of the reverse dielectric function of the medium accurate within a constant. The degree of coherency will then be

$$M(\chi) = \frac{\int\limits_0^{\min(k+k',q_{i\ max})} dq_i \quad \mathcal{G}_c(q_i,\omega,\chi)}{\int\limits_0^{\min(k+k',q_{i\ max})} dq_i \quad \mathcal{G}_L(q_i,\omega)}. \tag{33}$$

The function $\mathcal{G}_L$ determines the incoherent part of the electron cross section and takes the form

$$\mathcal{G}_L(q_i,\omega) = \frac{2\pi}{\gamma q_i} \left\{ \frac{1}{v} \left[\mathrm{tg}^{-1} \left(\frac{vq_i + \omega + \hbar q_i^2/2m}{\gamma} \right) + \mathrm{tg}^{-1} \left(\frac{vq_i - \omega - \hbar q_i^2/2m}{\gamma} \right) \right] + \right.$$
$$\left. + \frac{1}{v'} \left[\mathrm{tg}^{-1} \left(\frac{v'q_i + \omega - \hbar q_i^2/2m}{\gamma} \right) + \mathrm{tg}^{-1} \left(\frac{v'q_i - \omega + \hbar q_i^2/2m}{\gamma} \right) \right] \right\}. \tag{34}$$

The coherent part is determined by

$$\mathscr{G}_c(q_i,\omega,\chi)=\frac{4\pi}{q_i}\,\mathrm{Re}\left\{\mathscr{Y}^{-1}(v,v',\omega,\omega_c,\chi,q_i)\times\right.$$
$$\left.\times\log\left[\frac{q_i^2(\mathbf{vv}')+\left(\hbar q_i^2/2m\right)^2-\omega_c^2+q_i\mathscr{Y}}{q_i^2(\mathbf{vv}')+\left(\hbar q_i^2/2m\right)^2-\omega_c^2-q_i\mathscr{Y}}\right]\right\}, \tag{35}$$

where $\mathscr{Y}(v,v',\omega,\omega_c,\chi,q_i)$ has the form

$$\mathscr{Y}=\left\{\omega_c^2\left(\mathbf{v}-\mathbf{v}'\right)^2-\left[(q_i[\mathbf{vv}'])^2+\frac{2\hbar^2\omega\omega_c q_i^2}{m^2}-\left(\frac{\hbar q_i^2}{2m}\right)^2(\mathbf{v}+\mathbf{v}')^2\right]\right\}^{1/2}. \tag{36}$$

Here $\omega_c=\omega-i\gamma$.

The position of the angular features of the interference part in the electron cross section is mainly determined by zeros of the function $\mathscr{Y}$. The equation $\mathscr{Y}=0$ has two roots:

$$(q_i^2)_1=\frac{8\omega_c^2\left[[\mathbf{vv}']^2+(\hbar\omega/m)^2\right](\mathbf{v}+\mathbf{v}')^{-2}}{[\mathbf{vv}']^2+2\hbar^2\omega\omega_c m^{-2}+\sqrt{[\mathbf{vv}']^4+4\hbar\omega_c(\omega-\omega_c)m^{-2}[\mathbf{vv}']^2}}, \tag{37}$$

$$(q_i^2)_2=\frac{2m}{\hbar^2}\,\frac{[\mathbf{vv}']^2+2\hbar^2\omega\omega_c m^{-2}+\sqrt{[\mathbf{vv}']^4+4\hbar\omega_c(\omega-\omega_c)m^{-2}[\mathbf{vv}']^2}}{(\mathbf{v}+\mathbf{v}')^2}. \tag{38}$$

We can associate these roots with the value q_i defined by Eq. (19). The association is clearly seen in the limit of $\gamma\to 0$. In this case $\omega_c\to\omega$, and from Eq. (37) we obtain

$$q_{i_1}=\frac{2\omega}{\sqrt{|\mathbf{v}+\mathbf{v}'|^2}}. \tag{39}$$

Equation (39) coincides with Eq. (19). This means that the kinematic approach yields a reasonably good accuracy.

In the same approximation Eq. (38) yields

$$q_{i2}=\sqrt{\frac{k^4+k'^4-2k^2k'^2\cos 2\chi}{k^2+k'^2+2kk'\cos\chi}}. \tag{40}$$

From Eqs. (40), (18), and (19) we see the sum of Eq. (18) and the squared Eq. (19) is equal to the squared right-hand side of Eq. (40). Therefore, Eq. (40) corresponds to the case where $\mathbf{q}_i=\mathbf{Q}$. This solution is not significant for the new type of weak localization.

Since the equations are rather complicated and do not give a transparent insight into the dependence of the electron cross section on the various parameters, we present the theoretical features in Figs. 3–6 for a few typical cases.

Figure 3 shows $M(\chi)$ for the plasmon excitation in metals. Every curve shows a clearly defined slope. The nature of the sharp decrease has been explained in Sec. 2 on the basis of Eq. (22). In the case of a particular excitation the condition (22) might undergo some change. The dynamical approach takes into account these changes. In the particular case of the bulk plasmon excitation the change can be described in terms of the Čerenkov and bremsstrahlung generation of plasmons. The weak localization takes place when the plasmon

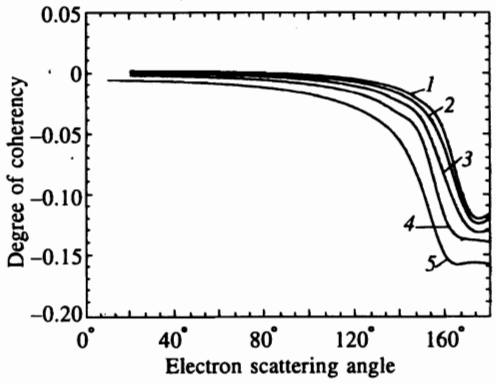

Fig. 3. Degree of coherency versus electron-scattering angle for plasmon excitation. The sharp decrease of the curves is due to the absence of the Čerenkov generation of plasmons. The difference in the degree of coherency from zero at angles which lie in the range from $2\cos^{-1}(v_F/v)$ up to π is due to the finiteness of γ and the contribution from the principal value in Eq. (5b). $\hbar\omega$ = = 10 eV, U' = 1 eV. Curve *1* corresponds to E = 200 eV, *2* — 300 eV, *3* — 400 eV, *4* — 500 eV, and *5* — 600 eV

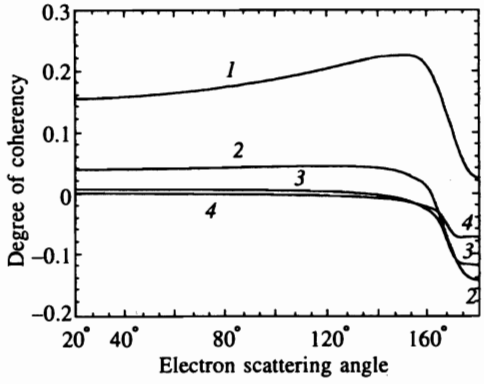

Fig. 4. Degree of coherency at different values of the energy loss. E = 500 eV, U' = 1 eV. Curve *1* corresponds to $\hbar\omega$ = 2 eV, *2* — 4 eV, *3* — 8 eV, and *4* — 12 eV

generation mechanism differs only slightly from the Čerenkov mechanism. The absence of the Čerenkov generation of plasmons at

$$2\cos^{-1}(v_F/v) < \chi < \pi$$

implies that at these angles the new type of weak localization is suppressed. The difference in the cross sections from zero at the angles which lie in the range from $2\cos^{-1}(v_F/v)$ up to π is due to the finiteness of γ and the contribution from the principal value in Eq. (5b).

Figure 4 shows the plot of $M(\chi)$ versus the energy loss due to the plasmon excitation. With an increase in $\hbar\omega_p$, the peak position shifts to smaller χ. If $\hbar\omega$ = 2 eV, the constructive interference takes place at $\chi_m = 150°$. If $\hbar\omega$ = 4 eV, we have $\chi_m = 120°$. These results agree with Eq. (21) which was obtained from a kinematic analysis.

The curves $M(\chi)$ depend also on the image potential. As shown in Fig. 5, a considerable decrease in the degree of coherency at $\chi = \pi$ (i.e., in the range of bremsstrahlung plasmon generation) takes place up to $\gamma/\omega = 0.5$. Only at $\gamma/\omega \simeq 1$ the angular dependence begins to smooth out when $\chi = 2\cos^{-1}(\omega/vq_i)$. In that case it looks like a peak on the curve $M(\chi)$. With an increase in γ, it shifts to $\chi = \pi$.

Figure 6 shows a theoretical curve $M(\chi)$ for excitation of polar optical phonons. Weak localization associated with this excitation corresponds to curve *5*. We assume that $\hbar\omega_{ph}$ = = 0.05 eV. Other curves correspond to $\hbar\omega_{ph}$ larger than for ordinary optical phonons. These curves show a variation of $M(\chi)$ when the energy loss increases from phonon to plasmon losses.

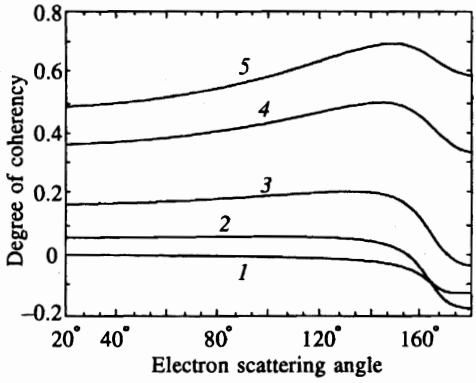

Fig. 5. Dependence of the degree of coherency on the image potential. $E = 500$ eV, $\hbar\omega = 10$ eV. Curve *1* corresponds to $U' = 1$ eV, *2* — 3 eV, *3* — 5 eV, *4* — 8 eV, and *5* — 10 eV

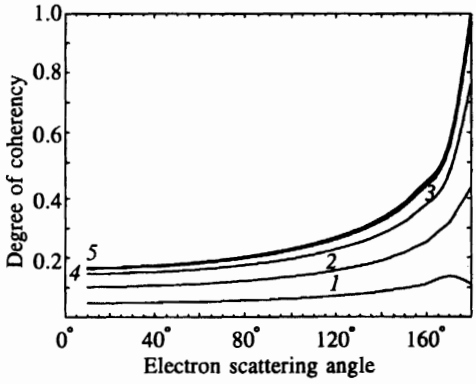

Fig. 6. Degree of coherency for quasielastic scattering. $E = 500$ eV, $U' = 1$ eV. Curve *1* corresponds to $\hbar\omega = 2$ eV, *2* — 1.0 eV, *3* — 0.5 eV, *4* — 0.2 eV, and *5* — 0.05 eV

At $\hbar\omega < 0.5$ eV, the width of the coherent peak at $\chi \simeq \pi$ is equal to 15° and it does not get narrower with a further decrease of $\hbar\omega$. This means that the weak localization of an electron during elastic scattering does not differ noticeably from the new type of weak localization during quasielastic scattering.

4. CONCLUSIONS

With a decrease in the energy loss, the new type of weak localization transforms into an ordinary weak localization. The transition is described by taking into account that the term $q_i^2/2m$ in the denominator of the Green's functions in Eq. (3) is more significant than $\hbar\omega$ in the limit $\omega \to 0$.

We have mentioned this fact at the end of Sec. 3. One can study the transition further by analyzing the variation of the ratio $\mathscr{G}_c/\mathscr{G}_L$ with $2m\omega/q_i^2$ at different scattering angles. The transition of the ordinary weak localization (i.e., at $\hbar\omega = 0$) to the new localization ($\hbar\omega \neq 0$) is shown in Fig. 7. For example, at $2m\omega q_i^{-2} = 0.8$ an announced maximum occurs for $\chi \simeq 175°$. The transition seems to take place for those $\hbar\omega$ and $q_i^2/2m$ which are $\geq \gamma$.

It can now be stated with assurance that we have explained why the angles typical of the new type of weak localization differ from π. The simple kinematic approach enables us to estimate these angles very accurately. The dependence of the angles on the electron energy loss and on

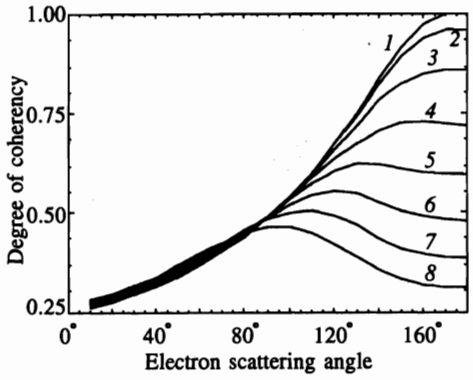

Fig. 7. Transition rate from ordinary weak localization to the new type of weak localization. $q_i^2/2mE = 0.01$, $q_c v/E = 0.2$, $\gamma/E = 0.01$. Curve *1* refers to $\hbar\omega = 0$, curve *2* corresponds to $\hbar\omega/E = 0.002$, *3* — 0.004, *4* — 0.006, *5* — 0.008, *6* — 0.010, *7* — 0.012, and *8* — 0.014

other parameters can be predicted. Finally, we have shown that there is no wall between new and ordinary weak localizations. The two phenomena are two different manifestations of the constructive quantum interference of electron waves.

We thank Prof. D. G. Yakovlev for critical reading of our paper and for helpful advice.

References

1. P. A. Lee and T. V. Ramakrishnan, Rev. Mod. Phys. **57**, 287 (1985).
2. G. Bergmann, Phys. Rep. **107**, 1 (1984).
3. J. Rammer, Rev. Mod. Phys. **63**, 781 (1991).
4. B. Kramer and A. MacKinnon, Rep. Prog. Phys. **56**, 1469 (1993).
5. A. Aronov, Phys. Scr. **49**, 28 (1993).
6. M. B. van der Mark, M. P. van Albada, and A. Lapendijk, Phys. Rev. **37**, 3575 (1988).
7. Y. A. Kravtsov, Rep. Prog. Phys. **55**, 39 (1992).
8. M. Kaveh, Physica B **175**, 1 (1991).
9. *Scattering and Localization of Classical Waves in Random Media*, ed. by P. Sheng, World Scientific, Singapore (1990).
10. R. Berkovits and M. Kaveh, Phys. Rev. B **37**, 584 (1988).
11. R. Berkovits, D. Eliyahu, and M. Kaveh, Phys. Rev. B **41**, 407 (1990).
12. E. E. Gorodnichev, S. L. Dudarev, and D. B. Rogozkin, Zh. Eksp. Teor. Fiz. **97**, 1511 (1990).
13. Jun-ichi Igarashi, Phys. Rev. B **35**, 8894 (1987).
14. M. Büttiker, Phys. Rev. B **32**, 1846 (1985).
15. M. Büttiker, Phys. Rev. B **33**, 3020 (1986).
16. Supriyo Datta, Phys. Rev. B **40**, 5830 (1989).
17. S. Washburn and R. A. Webb, Adv. Phys. **35**, 375 (1986).
18. L. P. Kanwenhoven, F. W. J. Hekking, B. J. van Wees, C. J. P. M. Harmans, C. E. Timmerling, and C. T. Foxon, Phys. Rev. Lett. **65**, 361 (1990).
19. F. Beltram, F. Capasso, D. L. Sivco, A. L. Hutchinson, S.-N. G. Chu, and A. Y. Chao, Phys. Rev. Lett. **64**, 3167 (1990).
20. V. Ambegoakar and U. Eckern, Phys. Rev. Lett. **65**, 381 (1990).
21. K. Maschke and M. Schreiber, Phys. Rev. B **44**, 3835 (1991).
22. J. L. D. D'Amato and H. M. Pastawski, Phys. Rev. B **41**, 7411 (1990).

23. E. A. Kanzieper, Zh. Eksp. Teor. Fiz. **103**, 1800 (1993); Phys. Scr. **47**, 823 (1993).
24. G. Bergmann, Wei Wei, Yao Zou, and R. M. Muller, Phys. Rev. B **41**; 7387 (1990).
25. P. W. Anderson, Philos. Mag. B **52**, 505 (1985).
26. V. Freilikher, M. Pustilnik, and I. Yurkevich, Phys. Rev. Lett. **73**, 810 (1994).
27. K. Maschke and M. Schreiber, Phys. Rev. B **49**, 2498 (1994).
28. R. L. Weaver, Phys. Rev. B **47**, 1077 (1993).
29. L. F. Rigister and K. Hess, Phys. Rev. B **49**, 1900 (1994).
30. S. John, Phys. Rev. Lett. **53**, 2169 (1984).
31. T. R. Kirkpatrick, Phys. Rev. B **31**, 5746 (1985).
32. C. A. Condat, J. Acoust. Soc. Amer. **83**, 441 (1988).
33. A. M. Jayannavar, Phys. Rev. B **49**, 14718 (1994).
34. M. Yosefin, Europhys. Lett. **25**, 675 (1994).
35. V. Freilikher, M. Pustilnik, and I. Yurkevich, Phys. Rev. B **50**, 6017 (1994).
36. L. Y. Gorelik, A. Grincwojg, V. Z. Kleiner, R. I. Shekhter, and M. Jonson, Phys. Rev. Lett. **73**, 2260 (1994).
37. B. N. Libenson, K. Yu. Platonov, and V. V. Rumyantsev, Zh. Eksp. Teor. Fiz. **101**, 614 (1992).
38. V. V. Rumyantsev and V. V. Doubov, Phys. Rev. B **49**, 8643 (1994).
39. E. V. Orlenko and V. V. Rumyantsev, J. Phys.: Condens. Matter **7**, 3557 (1995).
40. E. A. Kanzieper and V. Freilikher, Phys. Rev. B **51**, 2759 (1995).
41. E. A. Kanzieper, Phys. Rev. B **51**, 15563 (1995).
42. G. Bergmann, Phys. Rev. B **28**, 2914 (1983).